Cancer Chemother Pharmacol (2007) 60:423–435
DOI 10.1007/s00280-007-0490-z

ORIGINAL ARTICLE

Treatment parameters modulating regression of human melanoma xenografts by an antibody–drug conjugate (CR011-vcMMAE) targeting GPNMB

Vincent A. Pollack · Enrique Alvarez · Kam Fai Tse · Michael Y. Torgov · Sam Xie · Suresh G. Shenoy · John R. MacDougall · Sharon Arrol · Haihong Zhong · Robert W. Gerwien · William F. Hahne · Peter D. Senter · Michael E. Jeffers · Henri S. Lichenstein · William J. LaRochelle

Received: 23 January 2007 / Accepted: 30 March 2007 / Published online: 1 June 2007

Abstract
Purpose To investigate the pharmacological properties of the CR011-vcMMAE fully human antibody–drug conjugate (ADC), such as dose titrations, quantitation of the time (days) to complete regression, pharmacokinetics, and schedule dependency. Our prior study characterized a fully human antibody to GPNMB covalently linked to monomethylauristatin E, CR011-vcMMAE, and further demonstrated cell surface staining of melanoma lines susceptible to the immunoconjugate's cytotoxicity (Clin Cancer Res 2005; 12(4): 1373–1382).
Methods The human SK-MEL-2 and SK-MEL-5 melanoma xenografts were used in athymic mice to assess anti-tumor efficacy. After s.c. implantation, tumors became established (60–100 mg), and treatment commenced by i.v. injection of the immunoconjugate or vinblastine or paclitaxel. Short-term anti-tumor effects (inhibition of tumor growth) and long-term effects (complete regression) were observed.
Results CR011-vcMMAE induced regression of established human SK-MEL-2 and SK-MEL-5 xenografts at doses from 1.25 to 80 mg/kg treatment when administered intravenously every 4 days (4 treatments); strikingly, regressions were not associated with re-growth during the observation period (200 days). The disappearance rate of implants was dose dependent (minimum time, 18.5 days). Detectable serum CR011-vcMMAE ≥1 μg/mL (~0.01 μM) was observed for >30 days post-dose; CR011-vcMMAE showed an elimination half-life of 10.3 days. A low volume of distribution suggested that CR011-vcMMAE was confined to blood and interstitial fluid. CR011-vcMMAE could be delivered by either a single bolus dose or by intermittent dosing (i.e., every 1, 2, 4, 8, or 16 days) with no discernible differences in the proportion of tumor-free survivors, indicating a lack of schedule dependency. The antibody–drug conjugate produced complete regressions, but the equivalent doses of free monomethylauristatin E or unconjugated antibody did not show anti-tumor effects. In addition, decreases in plasma tumor-derived human interleukin-8 coincided with tumor nodule disappearance.
Conclusions Short-term anti-tumor effects and long-term effects (complete regression) were observed with CR011-vcMMAE, but not with the reference agents. These results suggest that CR011-vcMMAE may provide therapeutic benefit in malignant melanoma.

Keywords GPNMB · Melanoma · CR011-vcMMAE · Antibody–drug conjugate (ADC) · Xenograft

V. A. Pollack (✉) · E. Alvarez · K. F. Tse · M. Y. Torgov · S. Xie · S. G. Shenoy · J. R. MacDougall · S. Arrol · H. Zhong · R. W. Gerwien · W. F. Hahne · M. E. Jeffers · H. S. Lichenstein · W. J. LaRochelle
Department of Preclinical Development, CuraGen Corporation, 322 E. Main St, Branford, CT 06405, USA
e-mail: vpollack@curagen.com

P. D. Senter
Seattle Genetics, Inc, Bothell, WA, USA

Abbreviations

CR	Complete regression
C.V.	Coefficient of variation
GPNMB	Glycoprotein NMB
MMAE	Monomethylauristatin E
MTD	Maximum tolerated dose
ROA	Route of administration

Introduction

Malignant melanoma is a particularly aggressive form of cancer, and is by far the most life-threatening skin cancer. An estimated 62,190 people will be diagnosed in 2006 in the United States and 7,910 patients will succumb annually to the malignant form of this disease[1]. Despite extensive efforts to discover new chemotherapeutic agents, early detection has been the principal contributor to improved melanoma treatment, and thus melanoma presents a considerable unmet medical need [3].

Based on a large transcript differential display study, we identified GPNMB as a novel melanoma cell surface antigen with restricted distribution in non-tumorous tissues [42]. Human *gpnmb* was first described in a study of high and low metastatic human cell lines; two glycoproteins were associated with a low metastatic rate in the melanoma cell lines examined. We describe the glycoprotein ''non-metastatic b'' or GPNMB. The gene encodes a type 1a trans-membrane protein with closest amino acid sequence homology to melanocyte-specific protein, pMEL17 [46]. Orthologs of GPNMB include mouse DC-HIL [41], rat osteoactivin [35] and quail QNR-71 [25].

We have shown that GPNMB expression occurs in melanoma cell lines (7/7) and in a small sample of clinical specimens (5/5), using real time quantitative PCR. We extended these findings by examining a panel of 17 melanoma lines using semi-quantitative RT-PCR and found high expression in 15 of those lines, with weak expression in the amelanotic A-375 and no expression in the amelanotic LOXIMVI [45]. More recently, we examined GPNMB protein expressions by immunohistochemical staining with biotinylated CR011 and found that the majority (83%) of 58 clinical specimens express a moderate amount (i.e., ≥2+ intensity) of GPNMB protein [45]. We also showed that GPNMB is co-expressed with other melanoma-associated genes, such as MART-1, tyrosinase and pMEL-17.

In the melanoma cell lines tested, GPNMB expression was associated with antigen presentation at the membrane surface as determined by indirect FACS analysis with CR011 antibody [45]. Only melanoma cell lines that were positive for GPNMB transcript expression exhibited positive surface staining with CR011 antibody (i.e., ≥ 1.5-fold above the baseline staining by an isotype control IgG2 antibody). Flow cytometry also suggested that a portion of surface-bound CR011 was internalized following incubation. Nevertheless, the interaction of CR011 antibody alone with cell-surface GPNMB does not result in cytolysis in vitro or anti-tumor effects in vivo [45].

[1] US National Institutes of Health, Physicians Data Query, PDQ http://www.cancer.gov

Conjugation of CR011 with the anti-mitotic agent monomethylauristatin E provides an antibody–drug conjugate that potently inhibits cell growth of GPNMB-expressing tumor cells, but not cells that are negative by FACS analysis [45]. We have also shown that transfection of GPNMB non-expressing cells with a GPNMB vector confers susceptibility to inhibition and apoptosis, and conversely that GPNMB-expressing SK-MEL-2 cells exposed to siRNA do not show FACS positivity and are not growth inhibited in vitro. These observations suggest that CR011-vcMMAE is a GPNMB-specific antibody–drug conjugate (ADC) that may potently and effectively target the majority of melanoma tumors tested. The mechanism of action of the immunoconjugate is a multi-step process which involves: (1) binding to surface GPNMB and internalization [13, 45]; (2) enzymatic cleavage of the auristatin by cathepsin B [13]; (3) binding of auristatin to the *vinca* domain of β-tubulin [8, 34]; (4) inhibition of mitosis [13], and (5) subsequent apoptosis [13, reviewed by 47].

This paper describes the pharmacological properties of CR011-vcMMAE, such as the potency, magnitude and duration of anti-tumor effects, pharmacokinetics, and schedule dependency and correlates these observations with histological and systemic events accompanying the eradication of tumor cell deposits.

Materials and methods

Melanoma cell lines

SK-MEL-2 (ATCC #HTB-68) was derived from a metastatic site (skin of thigh) of a 60-year-old Caucasian male, and SK-MEL-5 (ATCC #HTB-70) from a metastatic site (axillary lymph node) of a 24-year-old Caucasian female [12].

Test animals

Five to 6-week-old athymic mice (NCr-*nu/nu* females) were obtained from Harlan Laboratories (Indianapolis, IN), and were housed in specific pathogen-free conditions, according to the guidelines of the Association for Assessment and Accreditation of Laboratory Animal Care International. Mice were provided sterilized pelleted food and filtered water ad libitum and kept in microisolator cages (6 mice/cage), which were changed twice weekly. Mice were housed in a room with conditioned ventilation (HVAC), temperature (22 ± 2°C), relative humidity (55 ± 15%), and photoperiod (12 h light/dark cycle). Studies were carried out with approved institutional animal care and use protocols. Mice were observed daily and clinical signs were noted.

Chemotherapy reference agents

Vinblastine sulfate (MF = $C_{46}H_{58}N_4O_9 \cdot H_2SO_4$; MW = 909.05 Da) was obtained as a dry powder (>97% by TLC) from Sigma-Aldrich (St Louis, MO) and was diluted with sterile phosphate-buffered saline immediately before use. Paclitaxel-reagent grade (MF = $C_{47}H_{51}NO_{14}$; MW = 853.9 Da) was obtained as a dry powder (>99%) from InB:Hauser Pharmaceuticals Cat. No. T016 (Denver, CO) and was diluted with sterile diluent immediately before use.

Preparation of CR011 monoclonal antibody

XenoMouse® technology was utilized for preparation of the monoclonal antibody (Abgenix Biopharma, Fremont, CA). Mice were immunized with soluble CG56972-03 protein, which encodes the extracellular domain and contains a novel 12 amino acid insertion. Subpopulations of B cells harvested from mice were fused with mouse myeloma cells to create hybridoma lines, which were screened for antibody production; the clone selected by cytotoxicity testing was CR011.1.15.1 [45].

RT-PCR was performed using oligo dT primers for first strand cDNA synthesis and heavy and light chain-specific primers for the PCR step. The forward primers contained the coding sequences for the secretion signal peptides as well as the first 10 codons of the mature heavy or light chain transcript. The amplicons were cloned into pCR2.1TOPO vector, and DNA sequences were verified. Next, the confirmed heavy and light chain cDNAs were subcloned into proprietary mammalian expression vectors pCTIMIL (for heavy chain) and pCTN (for light chain), and transfected into CHO-DG44 cells. Clones were selected for productivity (i.e., pg/cell/day) and growth characteristics.

The expression vectors were similar to the vectors HC and LC described by Aldrich [2]. For mammalian cells, both vectors utilize the cytomegalovirus enhancer/promoter, the adenovirus tripartite leader, the ECMV IRES, and the SV40 late polyadenylation site. Both vectors make a single transcript in mammalian cells that encodes a CR011 antibody chain and the selectable marker. The vectors utilize the ampicillin resistance gene and the origin of replication from the pUC119 to allow propagation in *E. coli*.

Preparation of the CR011-vcMMAE

CR011 bulk IgG2 antibody was buffer-exchanged into 50 mM borate, 50 mM NaCl pH 9.0 by diafiltration (10 diavolumes). Hinge region disulfides were partially reduced by tris(2-carboxyethyl) phosphine (Pierce Chemical Co., Rockford, IL) at 37°C for 3 h using 1:4.25 CR011 to TCEP ratio; the reaction was cooled to 4°C. Maleimidocaproyl-valine-citrulline-MMAE (vcMMAE, manufactured by Albany Molecular Research, Albany, NY) as 15 mg/mL solution in DMSO was added at 20% molar excess relative to the free thiols; additional DMSO was then added to a final concentration of 4% (v/v). The reaction was allowed to proceed for 1 h with gentle stirring. Unreacted vcMMAE was quenched with *N*-acetylcysteine (20 mol/mol maleimide) and the conjugate was purified by diafiltration into 10 volumes of 10 mM histidine, 10% (w/w) sucrose pH 6.0, and Tween-20 (0.02% final concentration), sterile filtered and stored at –80°C. The conjugate was analyzed for concentration by UV absorbance and aggregation by size-exclusion HPLC on TOSOH TSKgel SW3000 (7.5 × 30 mm). Drug/mAb molar ratios and percent of free vcMMAE were analyzed by reverse-phase HPLC using PLRP-S 1,000 Å column (2.1 × 50 mm) or Phenomenex Synergy Max RP 80 Å (4.6 × 150 mm), respectively. The resulting conjugate exceeded 99% monomeric protein. Drug/mAb molar ratio was 3.8; the level of free MMAE was <0.5%.

Human melanoma xenograft models

Anti-tumor effects were determined in athymic mouse xenograft models, according to published methods [14]. Test animals were implanted subcutaneously in the flank by trocar with 30–40 mg fragments excised from tumor donors. When tumors became established (10–20 days), mice were pair-matched into groups ($n = 6$ mice/group), and intravenous treatments were administered (tail vein injection). SK-MEL-2 and SK-MEL-5 have high ''take'' rates in immunocompromised hosts (97 and 93%, respectively) and low rates of spontaneous regression (3 and 0%, respectively) [11]. Xenograft studies with human tumors have been shown to effectively demonstrate anti-tumor effects for a variety of agents, which have subsequently shown activity against clinical cancer [15, 19, 38].

The effects of treatment were monitored by repeated tumor measurements across two diameters with Vernier calipers; tumor size (mg) was calculated using the formula, $(W^2 \times L)/2$, assuming a specific gravity of 1.0. Responses to treatment were further characterized by tumor growth inhibition (TGI) using the formula: TGI in % = $(TuS_{Controls} - TuS_{Test})/TuS_{Controls} \times 100\%$, where $TuS_{Controls}$ is the mean mass of pooled control groups and TuS_{Test} is that of the individual test groups; where multiple vehicles were employed, data from control groups were pooled and individual controls were then treated as test groups. Tumor size and body weights were assessed twice weekly. Moribund animals were euthanized humanely if clinical indications of excessive pain or distress were noted. Animals

with tumors exceeding 2,000 mg were removed from the study and euthanized.

Pharmacokinetics

Blood samples were collected from CO_2-anesthetized athymic mice (n = 3 mice/time point) by puncture of the retro-orbital plexus at various times post-dose and, after clotting, the serum was recovered by centrifugation and immediately stored at –20°C. In preliminary experiments we found that CR011-vcMMAE was stable in serum; less than 0.4% MMAE was released over 7 days incubation at 37°C. Nevertheless, serum samples were frozen immediately after collection, and assayed within 24 h of thawing.

A sandwich-type enzyme-linked immunosorbent assay (ELISA) was used to determine concentrations of CR011-vcMMAE in mouse serum. Briefly, microtiter wells were coated with 1 μg/mL GPNMB (CG56972-03) overnight at 4°C. Plates were blocked with buffer (Cat. No. 37515, Pierce, Rockford, IL) for 1 h at room temperature on a shaker. Plates were then washed three times with assay buffer containing 10% FBS (Cat. No. 555213, BD PharMingen, San Diego, CA), and serial dilutions of the samples and standards were added (100 μL/well in duplicate); plates were incubated 1 h at room temperature on a shaker. After washing three times, 100 μL/well of goat α-human IgG-horse radish peroxidase (HRP)-conjugate (1:20,000) was added (Cat. No. A80-319P, Bethyl Labs, Montgomery, TX), and plates were incubated for 1 h at room temperature on a shaker. After washing the plates, 100 μL/well of 3, 3′5, 5′-tetramethylbenzidine (TMB) substrate was added for 10 min. after which the reaction was stopped with 100 μL/well 1 N HCl. The plates were read at 450 nm and 630 nm (to correct for background); the calibration range for this assay was 2,000–1.98 ng/mL.

Histology

Tumor samples were excised from euthanized donors and central necrotic areas were dissected away; tissues were immediately preserved in 10% neutral buffered formalin at room temperature for 24 h and transferred to 70% ethanol before paraffin embedment. Sections of 5 μm were cut, mounted on microscope slides, and stained with hematoxylin and eosin according to standard procedures.

Human interleukin-8 quantitation

Interleukin-8 (IL-8) was measured by ELISA using a commercial kit (Human CXCL8/IL-8 Quantikine ELISA, 3rd Generation; R&D Systems, Minneapolis, MN), which recognizes human, but not mouse, IL-8. Interleukin-8 was detected by binding to IL-8-specific mAb pre-coated onto 96-well microtiter plates. Standards and samples were pipetted into wells and incubated for 2 h at room temperature. After washing, HRP-conjugated IL-8-specific polyclonal antibody was added to the wells and incubated for 1 h at room temperature. Following a wash, TMB substrate solution was added and color developed; the plate was read on an ELISA plate reader at 450 nm. Results were calculated from a standard curve using a four-parameter logistic curve fit. The lower limit of quantitation was 3.5 pg/mL and for each time point, n = 3 mice.

Biostatistics

Model validation compared animals treated with paclitaxel to saline vehicle controls, and the data were removed from further analysis. Median times to 2,000 mg were analyzed using the Kaplan–Meier method; inter-group differences were evaluated with a log-rank test [21]. Pair-wise comparisons between vehicle controls and individual groups were also based on a log-rank test without correction for multiplicity. Mass specific tumor growth rate (MSGR) was calculated as follows:

$$\text{MSGR} = \frac{\ln(S_f) - \ln(S_i)}{\Delta t}$$

where S_f and S_i are last measurable and initial tumor sizes, respectively, and Δt is the change in time. MSGR, also known as instantaneous growth rate, calculates growth rate while controlling for differences in initial tumor size. Data were analyzed with a one-way ANOVA using Dunnett's multiple comparison test. As with time to event data, the paclitaxel vs. saline control comparison was performed separately.

Results

Anti-tumor effects of CR011-vcMMAE vs. SK-MEL-2

SK-MEL-2 melanoma grows slowly and is unresponsive to conventional agents [11, 37]. We confirmed the slow growth of SK-MEL-2 (mean time to reach 1,000 mg = 38.4 days, C.V. = ± 9.6%, n = 7) and that it is unresponsive to treatment with the MTD of the following drugs: cisplatin, fluorouracil, BCNU, doxorubicin and vinblastine (data not shown). Only paclitaxel (15–24 mg/kg i.v. qd X5) had measurable anti-tumor effects in this model. We chose SK-MEL-2 as an early stage model because, like other melanomas, it expresses GPNMB at the cell surface [45]. CR011-vcMMAE shows potent cytotoxic effects in vitro (IC_{50} vs. SK-MEL-2 = 216 nM by clonogenic assay after 96 h exposure) [45].

CR011-vcMMAE produced substantial anti-tumor effects in a dose dependent manner (Fig. 1a). It significantly delayed tumor progression to 2,000 mg ($P = 2.17 \times 10^{-10}$, log-rank test) from a median of 52.5 days (95% CI: 49–∞) to an inestimable value at doses ≥1.25 mg/kg. Regression of established tumors occurred in the majority of animals at doses ≥1.25 mg/kg (see tabular insert for Fig. 1a); regressed tumors did not re-grow during the observation period (>200 days). Figure 1a also compares the anti-tumor effects of the CR011-vcMMAE conjugate with those of the reference agents vinblastine and paclitaxel, both of which were administered at the maximal tolerated doses as determined in preliminary experiments. Vinblastine produced a slight, but not significant, tumor growth inhibition ($P \leq 0.20$). Paclitaxel delayed tumor progression from a median of 52.5 days (49–∞) to 67 days (67–∞) when compared to saline controls ($P = 0.0033$). Significant growth inhibition and stasis (i.e., 100% growth inhibition) was observed for ~2 weeks after paclitaxel treatment ($P \leq 0.0077$). Despite this, tumors re-grew such that only one of six mice showed durable complete regression.

The time course for responsiveness to treatment is shown in Fig. 1b. Within 5 days after i.v. dosing, CR011-vcMMAE at the highest doses (i.e., 20 and 10 mg/kg) showed greater than 50% inhibition, whereas the lowest dose (i.e., 0.625 mg/kg) reached a point of 50% inhibition within ~10 days. These data suggested that the time required for tumor eradication by CR011-vcMMAE was related to dosage level. Figure 2 shows that, considering only the animals undergoing complete regressions, the time for dissolution of the tumor mass is dose dependent, with higher doses providing for more rapid tumor regression. The minimum time to 50% tumor growth inhibition was 6.0 days and that for complete regression was 18.5 days.

Over multiple experiments, CR011-vcMMAE showed reproducible dose dependent anti-tumor effects in the SK-MEL-2 melanoma model. The efficacious dose for tumor growth inhibition (ED_{50}) was a total dose of 2.00 mg/kg (CV, ± 35.4%) and the ED_{50} for complete regression a total dose of 4.59 mg/kg (CV, ± 44.4%) where $n = 4$ determinations.

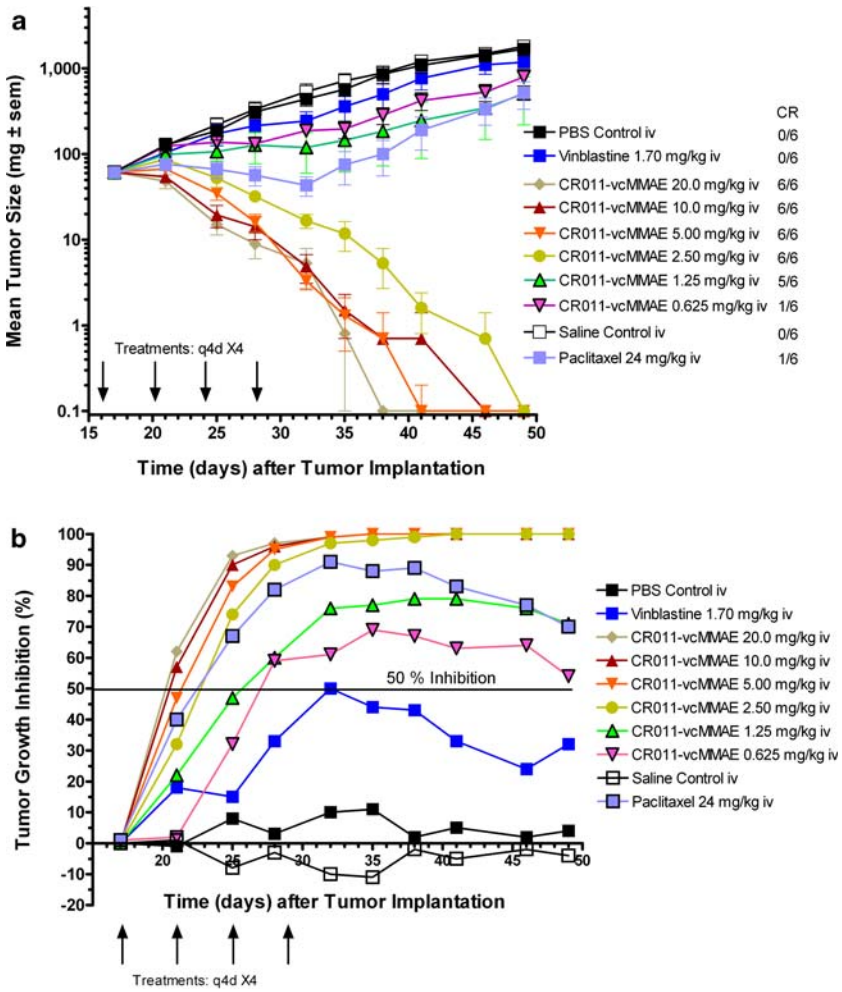

Fig. 1 **a** Established subcutaneous SK-MEL-2 tumors were treated on day 17 (mean tumor size = 61 mg) by intravenous injection of 0.10 mL/10 g body weight with a regimen of q4d X4 for all agents, except paclitaxel (q2d X4). For graphing purposes, animals showing complete regression (CR) were assigned nominal values of 0.1 mg before means were calculated. *Y*-values shown are mean tumor size in mg ± standard error of the mean. **b** Responsiveness to CR011-vcMMAE therapy is shown by plotting tumor growth inhibition as a function of time after tumor implantation; note rapid anti-tumor responses after the first treatment

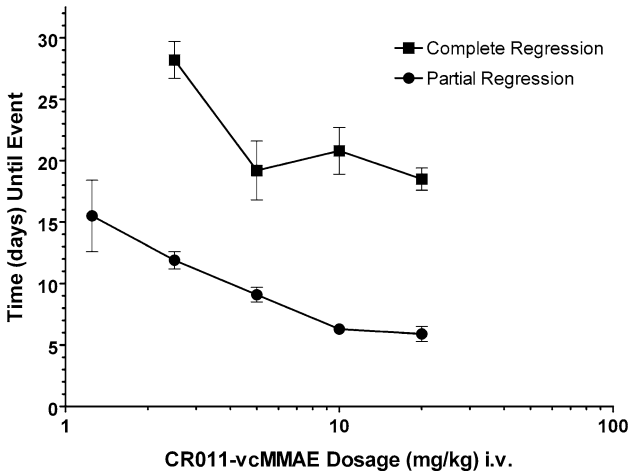

Fig. 2 Dose dependent partial and complete regression times induced by CR011-vcMMAE in the SK-MEL-2 xenograft model. For animals showing regression of SK-MEL-2 xenografts, the interval between first treatment and time (in days) until partial (50%) or complete regression was plotted as a function of the dosage level

The responses of SK-MEL-2 to CR011-vcMMAE therapy were readily detectable at the histological level. Within 24 h after i.v. administration of 10 mg/kg of CR011-vcMMAE, a high proportion of mitotic figures were evident amongst the tumor cells (data not shown); mitotic arrest is consistent with the mechanism of action of auristatin E and other dolastatin 10 analogues [20], and is consistent with the observed mode of action of CR011-vcMMAE in vitro [45]. At 48 h post-dose, tumors in animals treated with CR011-vcMMAE showed an increased level of cells with condensed, granular-appearing pyknotic nuclei with abundant eosinophilic cytoplasmic material, phenomena that were only minimally apparent in tumors treated with vehicle. These changes were much less evident at a lower, non-curative dosage level (i.e., 1 mg/kg), which more closely resembled the vehicle control tumors at early time points. At 4 days post-dose, H&E sections showed extensive killing of melanoma cells; only a few viable tumor cells could be seen amongst the majority of tumor cells. At 7 and 10 days post-dose, neither viable nor remnant non-viable tumor cells could be detected in the tumor bed by microscopy.

Anti-tumor effects of CR011-vcMMAE vs. SK-MEL-5

Though unrelated to SK-MEL-2 in origin, the SK-MEL-5 melanoma expresses GPNMB on the cell membrane surface and CR011-vcMMAE shows potent cytotoxic effects in vitro (IC_{50} = 300 nM) [45]. The anti-tumor effects of CR011-vcMMAE were examined in vivo (Fig. 3). Again, vinblastine produced a noticeable, but not significant, tumor growth inhibition ($P \leq 0.21$). Significant tumor growth inhibition was observed early after treatment with paclitaxel ($P \leq 0.039$, day 3) but was not as effective in this model as in the SK-MEL-2 xenografts. The responses of SK-MEL-5-bearing test animals to vinblastine and paclitaxel were short-lived, however. After cessation of treatment at the maximally tolerated doses, tumors resumed rapid, progressive growth. One long-term, tumor-free survivor occurred in the paclitaxel group and one

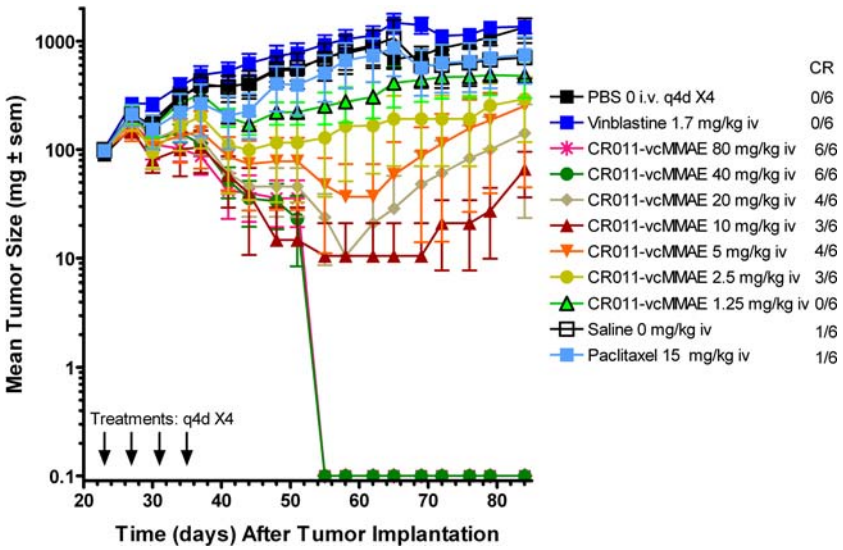

Fig. 3 Tumor size reduction and complete regression of SK-MEL-5 xenografts in athymic mice after treatment with CR011-vcMMAE at 1.25–20 mg/kg i.v. q4d X4. The responses of tumor-bearing animals to reference drugs vinblastine (1.7 mg/kg i.v. q4d X4) and paclitaxel (24 mg/kg i.v. q2d X4) are also shown. Control groups were treated with either 0.05 M phosphate-buffered saline pH 7.0 (PBS) or 0.85% NaCl (saline). For graphing purposes, animals showing complete regression of tumors were assigned nominal values for tumor size of 0.1 mg before means were calculated. *Y*-values shown are mean tumor size ± SEM

spontaneous regression occurred in the group treated with saline.

Substantial tumor growth inhibition, as well as tumor growth delay and complete regressions, occurred in SK-MEL-5 tumor-bearing animals after treatment with CR011-vcMMAE; the effects were dose dependent. At 10 mg/kg treatment, significant anti-tumor effects were noted as early as 7 days (the equivalent of 2 treatments) post-dose ($P \leq 0.0096$). CR011-vcMMAE produced tumor growth delay leading to complete regressions of established SK-MEL-5 melanoma xenografts (see tabular insert to Fig. 3). Complete regressions occurred at doses of as low as 2.5 mg/kg treatment, but not at 1.25 mg/kg treatment. No compound-induced toxicity was noted.

CR011-vcMMAE pharmacokinetics

The serum concentration-time profile for CR011-vcMMAE was determined in athymic mice after i.v. administration (Fig. 4a). Athymic mice receiving 1 or 10 mg/kg intravenously showed dose-proportional serum concentrations over the span of sampling times (42 days). The concentration-time pattern was bi-phasic. The initial phase (α), however, was minor as it contributed (<2% to the total area under the curve (AUC). Nevertheless, the compound disappeared very slowly from the peripheral blood ($T_{1/2}\beta$ = 10.3 days) with serum concentrations of 1 and 10 μg/mL, respectively, remaining in the blood for 6 weeks after dosing.

Pharmacokinetic parameters were estimated by fitting concentration–time data to a two-compartment open model with i.v. bolus input (Fig. 4b). One parameter is noteworthy. The volume of distribution at steady state (Vss) is very low, approaching the theoretical minimum; this suggests that the compound does not distribute outside the extravascular space. The distribution pattern, as well as the β-elimination phase for CR011-vcMMAE are in good agreement with values obtained for monoclonal antibodies in general (see Reviews by Mahmood and Green [28] or Lobo et al. [26]) and agree with values obtained for an antibody-MMAE conjugate with comparable drug loading [16].

Dosing interval study

The effects of timing on the anti-tumor effects of CR011-vcMMAE were examined by employing five different treatment intervals (i.e., 0, 1, 4, 8, or 16 days between treatments) and for each of these, three dosage levels were used to provide total doses of 2, 8, and 32 mg/kg CR011-vcMMAE (Table 1). For each dosing interval, the complete responses to CR011-vcMMAE were dose dependent. In addition, groups 2–4 showed that complete regressions

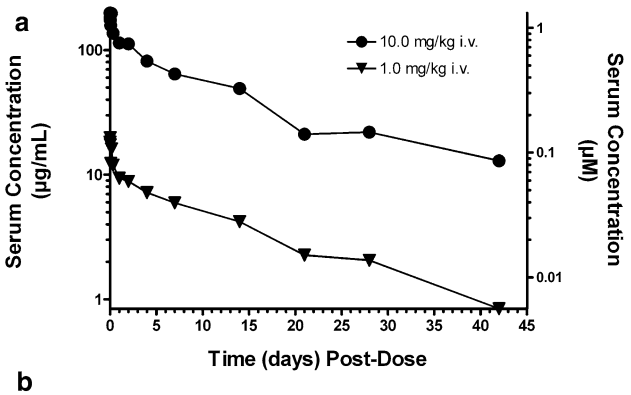

b

Parameter	Units	1 mg/kg	10 mg/kg
A	μg/mL	8.97	74.6
B	μg/mL	9.82	113
Alpha	1/h	0.179	0.0812
Beta	1/h	0.00269	0.00281
AUC	h* μg/mL	3,712	41,210
Alpha-Half Life	h	3.88	8.531
Beta-Half Life	h	258	247
Volume	mL/kg	53.2	53.2
Cmax	μg/mL	18.8	188
Cl	mL/h/kg	0.269	0.243
MRT	h	368	348
Vss	mL/kg	99.0	84.5

Fig. 4 **a** The serum concentration-time profile of the antibody component of CR011-vcMMAE after intravenous administration of 1 and 10 mg/kg in athymic mice (n = 3 mice/time point). Detection was achieved with a sandwich ELISA assay, which employed the CR011 antigen (CG56972-03, GPNMB) and a horseradish peroxidase-conjugated anti-human globulin. Results shown are the serum concentrations expressed as μg/mL (left Y-axis) and micromolar concentration (right Y-axis). **b** Pharmacokinetic parameters for CR011-vcMMAE. Abbreviations: *A* Pre-exponential constant for alpha phase, *Alpha* Exponential rate constant for alpha phase, *AUC* Total area under the curve from 0 to ∞, *B* Pre-exponential constant for beta phase, *Beta* Exponential rate constant for beta phase, *Cl* Total or systemic clearance, C_{max} Maximum observed concentration, *MRT* Mean residence time, *Volume* Volume of central compartment, *Vss* Steady-state volume of distribution

resulted after a single treatment (e.g., a dosing interval of 0). The aggregate responses for test animals responding to CR011-vcMMAE appear to suggest that bolus dosing and intervals of 1 and 4 days provide a slight advantage to the proportion of cures, compared to longer intervals, such as 8–16 days between doses (Fig. 5a); this effect, however, was not significant ($P < 0.2904$). These data suggest that the anti-tumor effects of CR011-vcMMAE are not schedule dependent. This conclusion is strengthened by the observation that test animals receiving a single bolus, which were exposed to plasma concentrations approximately fourfold higher than any of the other groups, did not show

Table 1 The effects of dosing interval on complete regressions after intravenous treatment with CR011-vcMMAE in athymic mice bearing s.c. SK-MEL-2 xenografts

Group	Treatment	Dosage level (mg/kg)	Regimen	Dosing interval (days)	Treatments (*n*)	Total dose (mg/kg)	Cures[a] (%)
1	PBS control	0	Bolus	0	1	NA	0
2	CR011-vcMMAE	32	Bolus	0	1	32	100
3		8	Bolus	0	1	8	83
4		2	Bolus	0	1	2	33
5	CR011-vcMMAE	8	qd X4	1	4	32	100
6		2	qd X4	1	4	8	100
7		0.5	qd x 4	1	4	2	17
8	CR011-vcMMAE	8	q4d X4	4	4	32	100
9		2	q4d X4	4	4	8	100
10		0.5	q4d X4	4	4	2	17
11	CR011-vcMMAE	8	q8d X4	8	4	32	100
12		2	q8d X4	8	4	8	100
13		0.5	q8d X4	8	4	2	0
14	CR011-vcMMAE	8	q16d X4	16	4	32	100
15		2	q16d X4	16	4	8	100
16		0.5	q16d X4	16	4	2	0
17	Excipients Control	0	q16d X4	16	4	NA	0

[a] Cures at 130 days post-implantation

any greater percentages of subjects undergoing complete regressions (e.g., compare groups 2–4 with groups 5–7).

The effects of dosage levels, in conjunction with various dosing intervals, are presented in Fig. 5b. Athymic mice receiving a total dose of 32 mg/kg showed complete regressions in 100% of each group, regardless of dosing interval; that is, a total dose of 32 mg/kg is schedule independent. Animals receiving 8 mg/kg total dose did not demonstrate schedule dependency either showing nearly the same proportions of complete regressions (i.e., 28/30 = 93%). Test animals receiving 2 mg/kg (total dose), which was recognized in preliminary studies to be below the threshold for cures (using a standardized regimen of q4d X4), appeared to be schedule dependent, though this was not significant, and produced a much lower proportion of complete regressors (i.e., 13%). These data also indicate that, in the SK-MEL-2 xenograft model, complete regression of established tumors can occur after a single bolus administration of CR011-vcMMAE.

Effects of CR011 monoclonal antibody and free MMAE compared to CR011-vcMMAE

Using the single i.v. treatment format described above, we compared the effects of free antibody and free MMAE to the CR011 conjugate in the SK-MEL-2 xenograft model (Table 2). The CR011 ADC showed dose dependent anti-tumor effects at a dose as low as 1.0 mg/kg i.v. for tumor growth inhibition and as low as 4.0 mg/kg i.v. for complete regression. No lethal toxicity or weight loss was observed with CR011-vcMMAE at the doses tested or with as much as 80 mg/kg of the compound in preliminary experiments (data not shown). Free monomethylauristatin E showed dose dependent anti-tumor effects as low as 0.576 mg/kg i.v. (tumor growth inhibition) and as low as 2.30 mg/kg i.v. for complete regressions. Unlike the CR011-vcMMAE conjugate, however, free MMAE showed dose dependent weight loss in these test animals measured 4 days after treatment (the body weight nadir for this compound); at 4.61 mg/kg i.v., MMAE demonstrated frank toxicity in 100% of the test animals. The CR011 monoclonal antibody (IgG2 subtype) produced no measurable therapeutic or observable toxic effects in this study and has not demonstrated anti-tumor effects at any dose in vivo to date.

The study in Table 2 was designed to evaluate the effects of free MMAE and unconjugated CR011 monoclonal antibody at doses that correspond to the proportions delivered by the intact conjugate. While CR011-vcMMAE showed dose dependent anti-tumor effects to the extent of producing complete regressions (i.e., doses from 4.0 to 16.0 mg/kg i.v.), it is also clear that the corresponding dosage levels of free MMAE showed no anti-tumor or toxic effects. Of course, at higher dosage levels of free MMAE (i.e., 0.576–2.30 mg/kg i.v.), we observed dose dependent anti-tumor effects, but in each case these were associated with dose dependent non-specific toxicity (e.g., weight loss).

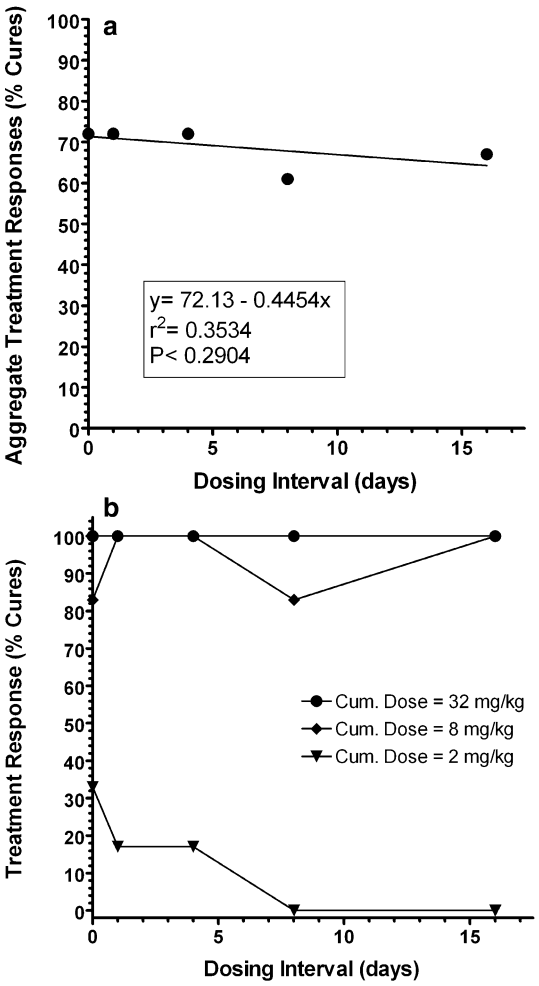

Fig. 5 **a** Aggregate responses, expressed as percent cures, were recorded for test animals treated with five different, graduated dosing intervals (i.e., 0, 1, 4, 8, and 16 days between each of 4 treatments). The slope of the line is not significantly different from 0 ($P < 0.2904$). **b** The proportions of complete regressors as a function of dosing interval and stratified by total dose. For each group, $n = 6$ mice. Athymic mice bearing established SK-MEL-2 tumor implants (day 14, 80 mg) were treated i.v. with CR011-vcMMAE by five different dosing intervals and the incidence of cures was recorded

SK-MEL-2 tumor-derived human IL-8 in plasma

Melanoma cells in culture produce a variety of signaling molecules [39, 4, 24] but they consistently secrete interleukin-8 [5], and this cytokine has been proposed as a surrogate marker of melanoma growth [7]. To examine whether plasma IL-8 might serve as a surrogate indicator of responses to therapy, mice bearing established SK-MEL-2 xenografts were dosed once with CR011-vcMMAE at 1 or 10 mg/kg doses, and a time course analysis of plasma human IL-8 determinations was monitored with an ELISA assay specific for human IL-8 (Fig. 6). Shortly before treatment (16 days after implantation), the human IL-8 in plasma was 29.8 pg/mL. At day 17.5 (1.5 days after treatment), plasma IL-8 in mice treated with 1 mg/kg CR011-vcMMAE increased to 46.3 pg/mL. IL-8 continued to increase throughout the experiment reaching 414.6 pg/mL on day 58 after tumor implantation (42 days after treatment); at this time, mean tumor size reached 2,000 mg and the test animals were euthanized. Human IL-8 in mice treated with 10 mg/kg reached 52.8 pg/mL by day 17.5 (1.5 days after treatment) and dropped to 24.39 pg/mL on day 23 (7 days after treatment). At ≥14 days after treatment, plasma IL-8 was undetectable. Mice treated with 10 mg/kg underwent complete regressions and no regrowths were observed. As expected, we did not detect human IL-8 in the plasma of normal (i.e., non-tumor bearing) mice. These data indicate that a decrease in plasma IL-8 correlates positively with a therapeutic response to CR011-vcMMAE and suggest that IL-8 may serve as a biomarker of effective treatment.

Discussion

CR011-vcMMAE produces potent anti-tumor effects against human melanoma both in vitro and in vivo [45]. In this report, we examined further its pharmacological properties such as the magnitude and duration of anti-tumor effects, pharmacokinetics, and schedule dependency and correlated these observations with the time course of tumor eradication. CR011-vcMMAE exhibited reproducible dose/response effects after i.v. administration in the SK-MEL-2 and SK-MEL-5 xenograft models. Pronounced anti-tumor effects in human xenograft models have been reported for auristatin E-based immunoconjugates (reviewed by [47]). Complete regressions were observed in the s.c. L2987 lung carcinoma and s.c. Karpas 299 lymphoma, using Lewis Y antigen- and CD30-specific immunoconjugates [10], respectively, and the data were confirmed and extended to the L540cy model of Hodgkin's lymphoma [13]. Tumor eradication was achieved with as little as 1–3 mg/kg treatment in these studies. Tumor growth inhibition was shown in carcinomas such as prostate [6] and colorectal [29] xenografts using E selectin (CD62E)-specific and EphB2-specific antibody drug conjugates, respectively, though complete regressions were not recorded. Anti-tumor effects sufficient to bring about complete regressions were subsequently shown in the s.c. LNCaP and s.c. CWR22 prostate xenograft models [1].

Pharmacokinetic parameters of CR011-vcMMAE were determined in athymic mice after intravenous administration. The data suggest that CR011-vcMMAE i.v. provides considerable exposure ($T_{1/2}$ = 10.3 days), and these results showed good agreement with previous reports [16] showing $T_{1/2}$ = 14.0 days for the cAC10-vcMMAE with drug loading of 4:1 and with subsequent data ($T_{1/2}$ = 11–17 days

Table 2 Comparison of the effects of equivalent single i.v. bolus doses of CR011-vcMMAE, monomethylauristatin E or unconjugated CR011 monoclonal antibody on anti-tumor effects and observable toxicity in athymic mice bearing s.c. xenografts of the human SK-MEL-2 melanoma

CR011-vcMMAE		MMAE		CR011 mAb	
Dosage (mg/kg)	Responses (efficacy/tox).	Dosage (mg/kg)	Responses (efficacy/tox).	Dosage (mg/kg)	Responses (efficacy/tox).
256	ND	4.61	Tox (100 %)[a] Wt. Loss 37%	251	ND
128	ND	2.30	CR (67%)[b], TGI Wt. Loss 21 %	126	ND
64.0	ND	1.15	No CR, TGI[c] Wt. Loss 8.9 %	62.8	ND
32.0	ND	0.576	No CR, TGI Wt. Loss 5.4 %	31.4	ND
16.0	CR (100%)	0.288	No effects[d]	15.7	No effects
8.00	CR (100%)	0.144	No effects	7.86	No effects
4.00	CR (67%), TGI	0.0720	ND	3.93	No effects
2.00	No CR, TGI	0.0360	ND	1.96	ND
1.00	No CR, TGI	0.0180	ND	0.982	ND
0.50	No effects	0.00900	ND	0.491	ND

Dose selection for free MMAE and unconjugated CR011 antibody was based on their molecular proportions in the intact CR011 conjugate. Note that for each row in the table, dosing of the MMAE and CR011 antibody corresponds to 1.8 and 98.2%, respectively, of the dosage of intact CR011-vcMMAE shown in the first column

ND not done

[a] Toxicity assessed by daily examination of test animals, and includes lethal toxicity and moribund animals, which were removed from the study and euthanized humanely. Numbers in parentheses indicate fraction of affected test animals, where $n = 6$ mice/group. Maximum mean weight loss (wt. loss), measured 4 days after compound administration is indicated only where it exceeds 5%

[b] Complete regression (CR) of s.c. tumor implant

[c] Tumor growth inhibition (i.e., ≥ 50% inhibition of tumor size relative to vehicle controls) recorded on two or more consecutive measurements. Data on PBS-treated and excipient-treated control groups not shown

[d] No effects, no observable toxicity or measurable anti-tumor effects

depending on Cys → Ser antibody variants at a stoichiometry of four drug molecules bound to 1 monoclonal antibody molecule) [31]. Additionally, the very low volume of distribution at steady state (i.e., close to the theoretical minimum) suggests that the ADC penetrates the vasculature and interstitial fluid, but probably not individual cells.

While the data presented here may have relevance for clinical applications, it should be noted that the CR011 antibody does not bind the mouse GPNMB protein expressed in normal mouse tissues (data not shown), and the in vivo therapy studies may therefore underestimate the toxicities and cross-reactivities of the ADC in a clinical setting. Further, the congenitally immunocompromised athymic mouse is unlikely to generate an antibody response or immunoregulatory responses (i.e., anti-idiotype responses), which could significantly affect pharmacokinetic exposure profiles and complicate comparison with immunocompetent species.

Initial studies employed four treatments with 4-day intervals, in order to compare our work with that of several preceding investigators. An analysis of dosing intervals from 0 interval (4 doses given as 1) to as long as 16-day intervals between treatments indicated no dependency of efficacy on treatment schedule. Further, groups that effectively received four doses as a single bolus administration showed the same proportions of complete regressors as the other sets of groups which were exposed to approximately one-fourth the peak plasma levels. As a result of this study, we view schedule dependency to be of lesser importance than total dose in determining the anti-tumor effects of CR011-vcMMAE.

Single bolus i.v. administration of CR011-vcMMAE was capable of inducing complete regressions. These results agree with recent studies of MMAE immunoconjugates in xenografted sarcomas [9, 16, 31, 44], and carcinomas such as the 786-0 renal carcinoma [18]. While it is tempting to speculate on the relevance of this observation to clinical dosing paradigms, the efficacy of single bolus administration is likely in these experimental studies to be due to the potency of CR011-vcMMAE as well as the absence of reactivity of CR011 antibody with endogenous mouse GPNMB. The clinical dosing regimen for CR011-vcMMAE therefore remains to be determined.

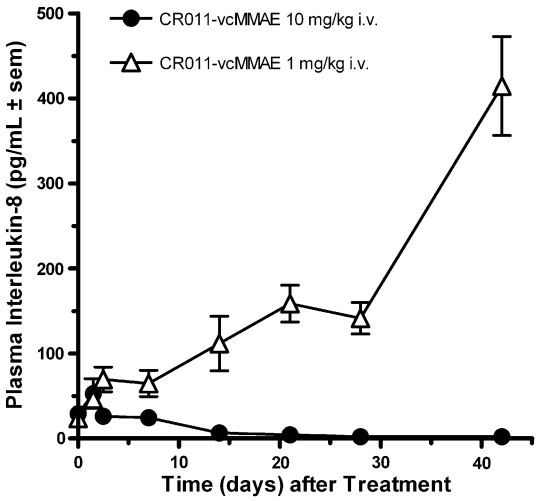

Fig. 6 Tumor-derived human IL-8 in mouse plasma. Results of kinetic analysis where groups of test animals bearing established SK-MEL-2 xenografts (n = 3 mice/time point treatment at 16 days post-implantation) were administered 1 mg/kg (non-curative) or 10 mg/kg (curative) of CR011-vcMMAE i.v. as a single bolus treatment and, at various times, plasma samples were taken. IL-8 was quantitated by a human IL-8-specific ELISA. Plasma IL-8 concentrations began falling 1.5 days after intravenous treatment with a curative dose (10 mg/kg), but not with an ineffective dose (1 mg/kg) of CR011-vcMMAE

Evaluation of the individual components of the CR011 ADC (i.e., free MMAE and unconjugated antibody) in the human melanoma xenograft model revealed that the unconjugated antibody, which comprises 98.2% of CR011-vcMMAE, completely lacked anti-tumor effects. These data agree with our previous data both in vitro and in vivo. At high doses, free MMAE showed dose dependent anti-tumor effects (i.e., tumor growth inhibition >50%) and complete regressions at the MTD (2.30 mg/kg i.v.). We also observed that there was co-associated non-specific toxicity (weight loss) at each therapeutically active dose. The anti-tumor effects from MMAE were anticipated because of its mode of action [45] and because of the known anti-tumor effects in xenograft models of analogues, such as dolastatin 10 [32], Auristatin PE [33] and TZT-1027 [22]. What was surprising, however, was that free MMAE dosage levels comparable to curative CR011-vcMMAE doses, were inactive in this melanoma xenograft model. These observations suggest that free MMAE is unlikely to contribute significantly to the efficacy of CR011-vcMMAE in the SK-MEL-2 xenograft model.

CR011-vcMMAE-induced toxicity, such as mortality or weight loss, was not observed despite the use of very high doses in the SK-MEL-2 melanoma xenograft (i.e., 20 mg/kg q4d X4 = total dose of 80 mg/kg) or with the SK-MEL-5 melanoma (i.e., 80 mg/kg i.v. q4d X4 = total dose of 320 mg/kg). Toxicity testing will require a non-rodent species, one that expresses the form of GPNMB recognized by the antibody (i.e., Cynomolgus monkey).

An interesting observation on the pharmacological properties of CR011-vcMMAE can be obtained in comparison with the anti-mitotic agents, vinblastine and paclitaxel. These drugs bind to, and inhibit, β-tubulin though at different molecular sites (reviewed in 17). Dolastatin 10 [36] and analogues such as dolastatin 15 [8], auristatin PE [36] and TZT-1027 [34] bind β-tubulin at the vinblastine-binding site and share the anti-mitotic mechanism of action. All three drugs are cytotoxic in vitro, but show disparate anti-tumor effects in the melanoma xenografts, ranging from noticeable, but non-significant activity (vinblastine) to substantial, non-curative anti-tumor activity (paclitaxel) to strong anti-tumor effects leading to complete regressions in the majority of treated animals (CR011-vcMMAE). Despite similarities in mechanism of action, a plausible explanation for the remarkable anti-tumor effects of CR011-vcMMAE is that vinblastine and paclitaxel lack the pharmacological drug delivery properties of the antibody component of CR011-vcMMAE, while sharing the same mechanism of action with the drug component of the ADC (i.e., MMAE). Further studies are ongoing to clarify this relationship.

The growth and development of melanoma in situ is a stepwise process involving an assortment of signaling macromolecules (i.e., cytokines), which facilitate cell division and tumor progression [27, 30]. Though these processes involve complex interactions amongst a variety of cytokines [4] melanoma cells tend to consistently secrete interleukin-8 [5]. Acting as an autocrine as well as paracrine growth factor, interleukin-8 stimulates melanoma cells to divide [40], to migrate [4] and to induce angiogenesis [23, 45]; further, secretion of interleukin-8 correlates with increased tumorigenicity and metastatic potential [17]. Taken together, the data suggest that interleukin-8 may serve as a biomarker of successful therapy of melanoma [7]. In the SK-MEL-2 model, human-specific plasma interleukin-8 levels decreased to undetectable amounts after effective therapy with 10 mg/kg i.v. CR011-vcMMAE, whereas in striking contrast IL-8 rose steadily to a high of 400 ng/mL in untreated control animals and in animals receiving a non-curative treatment (i.e., 1 mg/kg, 1 treatment only). That the plasma IL-8 was tumor-derived was evident because we could not detect human IL-8 in the plasma of non-tumor-bearing athymic mice. These initial observations suggest that plasma interleukin-8 determinations may provide a useful marker of successful immunotherapy with CR011-vcMMAE, but further studies are needed in order to implement this prognostic tool.

In summary, the pharmacological properties of the ADC CR011-vcMMAE suggest that this agent may have clinical utility in the control of human melanoma, a disease for which conventional chemotherapy has few effective agents.

Acknowledgments We wish to thank Michael Gallo and Gadi Gazit-Bornstein (Abgenix Biopharma, Fremont, CA), and Damon Meyer (Seattle Genetics, Inc., Bothell, WA) who contributed significantly to design of the ADC. For expertise in animal experimentation, we are grateful to Donald Dykes and Murray Stackhouse of Southern Research Institute (Birmingham, AL), as well as Michael Wick, Jennifer Marty and Marla Lear of the Institute for Drug Development (San Antonio, TX). We are also indebted to Bruce Mico for pharmacokinetic analysis, Steven Henck for helpful discussions and to Traci Mansfield for program management.

References

1. Afar DE, Bhaskar V, Ibsen E, et al (2004) Preclinical validation of anti-TMEFF2-auristatin E-conjugated antibodies in the treatment of prostate cancer. Mol Cancer Ther 3:921–932
2. Aldrich TL, Viaje A, Morris AE (2003) EASE vectors for rapid stable expression of recombinant antibodies. Biotechnol Prog 19:1433–1438
3. Atkins MB, Elder DE, Essner R, et al (2006) Innovations and challenges in melanoma: summary statement from the first Cambridge conference. Clin Cancer Res 12:2291s–2296s
4. Bar-Eli M (1999) Role of interleukin-8 in tumor growth and metastasis of human melanoma. Pathobiology 67:12–18
5. Bennicelli JL, Guerry Dt (1993) Production of multiple cytokines by cultured human melanomas. Exp Dermatol 2:186–190
6. Bhaskar V, Law DA, Ibsen E, et al (2003) E-selectin up-regulation allows for targeted drug delivery in prostate cancer. Cancer Res 63:6387–6394
7. Brennecke S, Deichmann M, Naeher H, Kurzen H (2005) Decline in angiogenic factors, such as interleukin-8, indicates response to chemotherapy of metastatic melanoma. Melanoma Res 15:515–522
8. Cruz-Monserrate Z, Mullaney JT, Harran PG, Pettit GR, Hamel E (2003) Dolastatin 15 binds in the vinca domain of tubulin as demonstrated by Hummel–Dreyer chromatography. Eur J Biochem 270:3822–3828
9. Doronina SO, Mendelsohn BA, Bovee TD, Cerveny CG, Alley SC, Meyer DL, Oflazoglu E, Toki BE, Sanderson RJ, Zabinski RF, Wahl AF, Senter PD (2006) Enhanced activity of monomethylauristatin F through monoclonal antibody delivery: effects of linker technology on efficacy and toxicity. Bioconjug Chem 17:114–124
10. Doronina SO, Toki BE, Torgov MY, et al (2003) Development of potent monoclonal antibody auristatin conjugates for cancer therapy. Nat Biotechnol 21:778–784
11. Dykes DJ, Abbott BJ, Mayo JG, et al (1992) Development of human tumor xenograft models for in vivo evaluation of new antitumor drugs. In: Fiebig HH, Berger DP (eds) Immunodeficient mice in oncology. Contrib Oncol, vol 42. Karger, Basel, pp 1–22
12. Fogh J, Fogh JM, Orfeo T (1977) One hundred and twenty-seven cultured human tumor cell lines producing tumors in nude mice. J Natl Cancer Inst 59:221–226
13. Francisco JA, Cerveny CG, Meyer DL, et al (2003) cAC10-vcMMAE, an anti-CD30-monomethyl auristatin E conjugate with potent and selective antitumor activity. Blood 102:1458–1465
14. Geran RI, Greenberg NH, Macdonald MM, Schumacher AM, Abbott BJ (1972) Protocols for screening chemical agents and natural products against animal tumors and other biological systems. Cancer Chemother Rep 3:1–104
15. Gitler MS, Sausville EA, Hollingshead M, Shoemaker R (2004) In vivo models for experimental therapeutics relevant to human cancer. Cancer Res 64:8478–8480
16. Hamblett KJ, Senter PD, Chace DF, et al (2004) Effects of drug loading on the antitumor activity of a monoclonal antibody drug conjugate. Clin Cancer Res 10:7063–7070
17. Huang S, DeGuzman A, Bucana CD, Fidler IJ (2000) Nuclear factor-kappaB activity correlates with growth, angiogenesis, and metastasis of human melanoma cells in nude mice. Clin Cancer Res 6:2573–2581
18. Jeffrey SC, Andreyka JB, Bernhardt SX, Kissler KM, Kline T, Lenox JS, Moser RF, Nguyen MT, Okeley NM, Stone IJ, Zhang X, Senter PD (2006) Development and properties of beta-glucuronide linkers for monoclonal antibody–drug conjugates. Bioconjug Chem 17:831–840
19. Johnson JI, Decker S, Zaharevitz D, et al (2001) Relationships between drug activity in NCI preclinical in vitro and in vivo models and early clinical trials. Br J Cancer 84:1424–1431
20. Jordan MA, Wilson L (2004) Microtubules as a target for anticancer drugs. Nat Rev Cancer 4:253–265
21. Kaplan EL, Meier P (1958) Nonparametric estimation from incomplete observations. J Am Statistical Assoc 53:457–481
22. Kobayashi M, Natsume T, Tamaoki S, Watanabe J, Asano H, Mikami T, Miyasaka K, Miyazaki K, Gondo M, Sakakibara K, Tsukagoshi S (1997) Antitumor activity of TZT-1027, a novel dolastatin 10 derivative. Jpn J Cancer Res 88:316–327
23. Koch AE, Polverini PJ, Kunkel SL, et al (1992) Interleukin-8 as a macrophage-derived mediator of angiogenesis. Science 258:1798–1801
24. Lazar-Molnar E, Hegyesi H, Toth S, Falus A (2000) Autocrine and paracrine regulation by cytokines and growth factors in melanoma. Cytokine 12:547–554
25. Le Borgne R, Planque N, Martin P, Dewitte F, Saule S, Hoflack B (2001) The AP-3-dependent targeting of the melanosomal glycoprotein QNR-71 requires a di-leucine-based sorting signal. J Cell Sci 114:2831–2841
26. Lobo ED, Hansen RJ, Balthasar JP (2004) Antibody pharmacokinetics and pharmacodynamics. J Pharm Sci 93:2645–2668
27. Lu C, Kerbel RS (1994) Cytokines, growth factors and the loss of negative growth controls in the progression of human cutaneous malignant melanoma. Curr Opin Oncol 6:212–220
28. Mahmood I, Green MD (2005) Pharmacokinetic and pharmacodynamic considerations in the development of therapeutic proteins. Clin Pharmacokinet 44:331–347
29. Mao W, Luis E, Ross S, et al (2004) EphB2 as a therapeutic antibody drug target for the treatment of colorectal cancer. Cancer Res 64:781–788
30. Mattei S, Colombo MP, Melani C, Silvani A, Parmiani G, Herlyn M (1994) Expression of cytokine/growth factors and their receptors in human melanoma and melanocytes. Int J Cancer 56:853–857
31. McDonagh CF, Turcott E, Westendorf L, et al (2006) Engineered antibody–drug conjugates with defined sites and stoichiometries of drug attachment. Protein Eng Des Sel 19(7):299–307
32. Miyazaki K, Kobayashi M, Natsume T, Gondo M, Mikami T, Sakakibara K, Tsukagoshi S (1995) Synthesis and antitumor activity of novel dolastatin 10 analogs. Chem Pharm Bull (Tokyo) 43:1706–1718
33. Mohammad RM, Varterasian ML, Almatchy VP, Hannoudi GN, Pettit GR, Al-Katib A (1998) Successful treatment of human chronic lymphocytic leukemia xenografts with combination biological agents auristatin PE and bryostatin 1. Clin Cancer Res 4:1337–1343
34. Natsume T, Watanabe J, Tamaoki S, Fujio N, Miyasaka K, Kobayashi M (2000) Characterization of the interaction of TZT-1027, a potent antitumor agent, with tubulin. Jpn J Cancer Res 91:737–747
35. Owen TA, Smock SL, Prakash S, et al (2003) Identification and characterization of the genes encoding human and mouse osteoactivin. Crit Rev Eukaryot Gene Expr 13:205–220

36. Pettit GR, Srirangam JK, Barkoczy J, et al (1995) Antineoplastic agents 337. Synthesis of dolastatin 10 structural modifications. Anticancer Drug Des 10:529–544
37. Plowman J, Dykes DJ, Hollingshead M, Simpson-Herren L, Alley MC (1997) Human tumor xenograft models in NCI drug development Anticancer drug development guide: preclinical screening, clinical trials, and approval. In: Teicher B (ed) Humana Press, Totowa, pp 102–125
38. Pollack VA, Savage DM, Baker DA, et al (1999) Inhibition of epidermal growth factor receptor-associated tyrosine phosphorylation in human carcinomas with CP-358,774: dynamics of receptor inhibition in situ and antitumor effects in athymic mice. J Pharmacol Exp Ther 291:739–748
39. Rodeck U (1993) Growth factor independence and growth regulatory pathways in human melanoma development. Cancer Metastasis Rev 12:219–226
40. Schadendorf D, Moller A, Algermissen B, Worm M, Sticherling M, Czarnetzki BM (1993) IL-8 produced by human malignant melanoma cells in vitro is an essential autocrine growth factor. J Immunol 151:2667–2675
41. Shikano S, Bonkobara M, Zukas PK, Ariizumi K (2001) Molecular cloning of a dendritic cell-associated transmembrane protein, DC-HIL, that promotes RGD-dependent adhesion of endothelial cells through recognition of heparan sulfate proteoglycans. J Biol Chem 276:8125–8134
42. Shimkets RA, Lowe DG, Tai JT, et al (1999) Gene expression analysis by transcript profiling coupled to a gene database query. Nat Biotechnol 17:798–803
43. Strieter RM, Kunkel SL, Elner VM, et al (1992) Interleukin-8. A corneal factor that induces neovascularization. Am J Pathol 141:1279–1284
44. Sun MM, Beam KS, Cerveny CG, Hamblett KJ, Blackmore RS, Torgov MY, Handley FG, Ihle NC, Senter PD, Alley SC (2005) Reduction–alkylation strategies for the modification of specific monoclonal antibody disulfides. Bioconjug Chem 16:1282–1290
45. Tse KF, Jeffers M, Pollack VA, et al (2006) CR011, a fully human monoclonal antibody-auristatin E conjugate, for the treatment of melanoma. Clin Cancer Res 12:1373–1382
46. Weterman MA, Ajubi N, van Dinter IM, et al (1995) nmb, a novel gene, is expressed in low-metastatic human melanoma cell lines and xenografts. Int J Cancer 60:73–81
47. Wu AM, Senter PD (2005) Arming antibodies: prospects and challenges for immunoconjugates. Nat Biotechnol 23:1137–1146